1 **Thermoplastic cassava starch-chitosan bilayer films containing essential oils**

2 Cristina Valencia-Sullca, María Vargas*, Lorena Atarés, Amparo Chiralt

3 Instituto de Ingeniería de Alimentos para el Desarrollo, Universitat Politècnica de

4 València

5 *mavarco@tal.upv.es

6

7 **Abstract**

8 Starch-chitosan bilayer films, containing or not essential oils in the casted chitosan

9 layer were obtained by thermo-compression. Bilayer films exhibited a good interfacial

10 adhesion and better mechanical resistance than starch monolayers, although they

11 were less stretchable and less transparent. Starch-chitosan films were effective at

12 controlling the bacterial growth in pork meat, but the thermal treatment applied to

13 obtain the bilayers reduced their antimicrobial properties as compared to chitosan

14 monolayers. The addition of essential oils did not promote any antimicrobial action in

15 chitosan mono and bilayer films applied to pork meat. The final amount of essential oils

16 in the films was very limited probably due to the losses occurred during film processing

17 method. Other strategies to incorporate the essential oils into chitosan-based films

18 should be used to improve their final retention in the film matrix and their effective

19 release into the coated food.

20

22

23 **1.   Introduction**

24 In recent years, the interest in biodegradable films has grown mainly due to general

25 concern about the disposal of conventional synthetic plastic materials since their full

26 degradation generally requires a long period of time (Xu, Kimb, Hanna, & Nag, 2005).

27 Starch has been considered for many years as a biodegradable polymer with a high

28 potential for packaging applications (Doane, Swanson, & Fanta, 1992; Shogren, 1998).

29   Biodegradable films based on hydrocolloids such as starch can act as barriers to

30   control the transfer of moisture, oxygen, carbon dioxide, lipids, and flavor components,

31   thus preventing quality deterioration and increasing the shelf-life of food products

32   (Ghanbarzadeh & Oromiehi, 2009; Naushad Emmambux & Stading, 2007). The use of

33   starch from different sources (corn, cassava, wheat, rice, potato, pea, etc.) to obtain

34   biodegradable plastics is being extensively studied since starch is abundant and

35   accessible at a relatively low cost (Mali, Grossmann, García, Martino, & Zaritzky, 2006;

36   Khan, Bilal Khan Niazi, Samin, & Jahan, 2017), Thermoplastic Starch: A Possible

37   Biodegradable Food Packaging Material—A Review. Journal of Food Process

38   Engineering, 40: n/a, e12447. doi:10.1111/jfpe.12447). Several authors have shown

39   the possibility to transform native starch into thermoplastic-like products under

40   restructuring and plasticization conditions (Swanson, Shogren, Fanta, & Imam, 1993).

41   Furthermore, the feasibility of processing starch by using plastic-processing equipment

42   has long been demonstrated (Tomka, 1991).

43   Thermoplastic starch (TPS) can be processed in the same way as synthetic plastics

44   through extrusion and injection units (Avérous, Moro, Dole, & Fringan, 2000) and

45   thermocompression (Flores, Costa, Yamashita, Gerschenson, & Grossmann Eiras,

46   2010; Pellissari, Grossmann, Yamashita, & Pineda, 2012; Thunwall, Boldizar, &

47   Rigdahl, 2006). The thermocompression method is useful as a processing method

48   because of its simplicity and capability of producing films (López et al. 2014). During

49   the extrusion of starch, the combination of shear, temperature and plasticizers allows

50   for producing a molten thermoplastic material by disruption of the native crystalline

51   granular structure and plasticization. This plasticized starch could be suitable for

52   injection molding or thermoforming (Avérous, Fringan & Moro, 2001). TPS is a very

53   hydrophilic product (Avérous et al., 2000) and yields films with high water sensitivity

54   (Zobel, 1988) and poor mechanical properties (Van Soest, 1996), which change with

55   time (crystallization due to ageing and plasticization by water adsorption). The

56   combination of starch with chitosan (CH) led to the improvement of the functional

57   properties of the films while conferring them antimicrobial properties (Bonilla, Vargas,

58   Atarés, & Chiralt, 2014).

59   Chitosan is a biodegradable biopolymer that has shown excellent properties such as

60   bio-compatibility, non-toxicity and adsorption to negatively charged interfaces since it is

61   positively charged in acid media (Dutta, Dutta, & Tripathi, 2004; Lertsutthiwong, Ng,

62   Chandrkrachang, & Stevens, 2002; Rizzi, & Pinto, 2007; Weska, Moura, Batista, Youn,

63   No, & Prinyawiwatkul, 2007).

64   The use of films as carriers of antimicrobial agents, such as essential oils, represents

65   an interesting approach for the external incorporation of such active ingredients onto

66   food system surfaces. Essential oils, which exhibit both antimicrobial and antioxidant

67   capacity (Bakkali, Averbeck, Averbeck, & Idaomar, 2008), were incorporated into the

68   formulation of antimicrobial films based on chitosan to extend the shelf-life of minced

69   pork meat (Bonilla et al., 2014). Oregano essential oil (OEO) has been shown to

70   possess higher antimicrobial activity than other essential oils such as thyme or basil

71   essential oil (Burt, 2004), and it has been effective at inhibiting the microbial growth of

72   some foodborne microorganisms, such as *Staphylococcus aureus*, *Escherichia coli* and

73   *Bacillus subtilis* (Lv, Liang, Yuan, & Li, 2011). Carvacrol, the main compound of OEO,

74   was effective in inhibiting the growth and survival of *Listeria monocytogenes*,

75   *Aeromonas hydrophila*, and *Pseudomonas fluorescens* (de Sousa et al. 2012).

76   Cinnamon leaf essential oil (CLEO) is recognized for its aroma and medicinal

77   properties (Ayala-Zavala et al., 2008; Singh, Srivastava, Singh, & Srivastava, 2007).

78   The main component of CLEO is eugenol (70-95%), followed by cinnamaldehyde,

79   which can be present in a proportion of 1-5% (Vangalapati, Satya, Prakash, &

80   Avanigadda, 2012). In addition, CLEO antimicrobial and antifungal properties have also

81   drawn great attention in many studies (Chang, Chen, & Chang, 2001; Kim, Park, &

82   Park, 2004; Park, Lee, Lee, Park, & Ahn, 2000; Singh et al., 1995). Essential oils and

83   their active ingredients can diffuse from the film into the coated food to control target

84   microorganisms. In this sense, the combination of biodegradable polymers (Starch-

85 CH) as bilayers, where CH encapsulates the antimicrobial agent and is not submitted

86 to the heat blending step, can be an interesting approach to obtain new biodegradable

87 films with antimicrobial activity. However, there are not previous studies on the

88 development of these type of bilayer films, to the best of our knowledge.

89 The aim of this work was to characterize the thermal behavior, optical, barrier,

90 mechanical and antimicrobial properties of bilayer films prepared with thermoplastic

91 starch and chitosan, containing or not oregano or cinnamon leaf essential oil in the

92 chitosan layer.

93

94 **2. Materials and methods**

95

96 2.1. Materials

97 Cassava starch was supplied by Quimidroga S.A. (Barcelona, Spain), high molecular

98 weight chitosan (practical grade, >75% deacetylation degree, Batch MKBP1333V),

99 polyethylene glycol (PEG), Tween 85 and Glycerol (Gly) were supplied by Sigma-

100 Aldrich (Madrid, Spain). Oregano (OEO) and cinnamon leaf (CLEO) essential oils were

101 provided by Herbes del Molí (Alicante, Spain) and $Mg(NO_3)_2$ was obtained from

102 Panreac Química, S.A. (Castellar del Vallés, Barcelona, Spain). Pork meat, which was

103 used for the microbiological study, was purchased in a local supermarket. Tryptone

104 Phosphate Water (peptone buffered water), Violet Red Bile Agar (VRB agar) and Plate

105 Count Agar (PCA) were provided by Scharlau Microbiology (Barcelona, Spain).

106

107 2.2. Film preparation

108 Chitosan-based films were obtained by casting as previously described by Bonilla et al.

109 (2014). Chitosan (1.0% w/w) was dispersed in an aqueous solution of glacial acetic

110 acid (1.0% v/w) under magnetic stirring at 40 ºC for 24 h. The film-forming dispersions

111 (FFDs) were obtained by adding OEO or CLEO at 0.25 % (w/w) and Tween 85 at 0.1

112 % (w/w). FFDs were homogenized with a rotor-stator (13500 rpm, 4 min, Yellow Line

4

113 DL 25 Basic, IKA, Janke y Kunkel, Germany) and degassed at room temperature with

114 a vacuum pump. Subsequently, FFDs were cast in a framed and leveled

115 polytetrafluorethylene (PTFE) plate (diameter = 15 cm, 5.6 mg solids/cm^2) and dried at

116 room temperature at 45% relative humidity RH. Sample codes for chitosan films, with

117 or without OEO and CLEO were: CH, CH:OEO and CH:CLEO.

118 Cassava starch films (CS) were obtained by melt blending and compression molding.

119 Thermoplastic CS pellets were obtained by melt blending in a roll-mill (Model LRM-M-

120 100, Labtech Engineering, Thailand) at 160ºC for 30 min with the plasticizer blend

121 (glycerol:PEG) at 30 % with respect to the starch, and 24% of water, which evaporates

122 during the process. Polymer: plasticizer mass ratio was 1:0.3 and Gly: PEG mass ratio

123 was 3:0.05. The pellets were conditioned at 53% RH and they were submitted to

124 compression molding with a hot plates hydraulic press (Model LP20, Labtech

125 Engineering, Thailand) at 160 ºC and 1.2 x 10^7 Pa. This film was named as CS.

126 Chitosan-starch bilayer films were obtained by compressing CS film and chitosan

127 based films, at 100 ºC for 2 min by means of the hot-plates hydraulic press. The

128 obtained bilayer films were named as follows: CS-CH; CS-CH:OEO and CS-CH:CLEO.

129 Taking into account the relative weight of each layer with the same area, the ratio S:CH

130 was 3:1.

131 All films were stored at 25 ºC and 53% RH for one week prior performing the analysis

132 of thermal, barrier, optical and mechanical properties. Film thickness was measured

133 using a Palmer digital micrometer (Comecta, Barcelona, Spain) to the nearest 0.001

134 mm. Six to eight random positions in each film sample were considered.

135

136 2.3. Field emission scanning electron microscopy

137 The microstructural analysis of the cross-sections of the bilayer films was carried out by

138 means of a field emission scanning electron microscope (Ultra 55, Zeiss, Cambridge,

139 UK). The film samples were maintained in desiccators with P_2O_5 to guarantee that

140 water was not present in the sample and two samples per film formulation were

141 analyzed. Film pieces, 0.5 cm^2 approximately in size, were cryofractured from films and

142 fixed on copper stubs, gold coated, and observed using an accelerating voltage of 2

143 kV.

144

145 2.4. Thermogravimetric analysis

146 A thermogravimetric analyzer (TGA/SDTA 851e, Mettler Toledo, Schwerzenbach,

147 Switzerland), equipped with an ultra-micro weighing scale (± 0.1 µg), was used to

148 determine the thermal stability of the film samples under nitrogen flow (50 mL/min). The

149 analysis was carried out using the following temperature program: heating from 25 to

150 600 ^{o}C at a 10 ^{o}C/min heating rate. Approximately 3 mg of each sample were used in

151 each test, considering at least two replicates for each one. Initial degradation

152 temperature (T_0) and the temperature of the maximum degradation rate (T_{max}), were

153 registered from the first derivative of the resulting weight loss curves.

154

155 2.5. Mechanical properties

156 Mechanical properties were measured with a Universal Test Machine (TA.XT plus,

157 Stable Micro Systems, Haslemere, England), following the ASTM standard method

158 D882 (ASTM, 2001). Equilibrated film samples (25 mm wide and 100 mm long) were

159 mounted in the film-extension grips (A/TG model), which were set 50 mm apart.

160 Tension test was performed at 50 mm/min. Stress-strain curves were obtained and the

161 tensile strength at break (TS), percentage of elongation at break (ε) and elastic

162 modulus (EM) were calculated. Ten replicates carried out per formulation.

163

164 2.6. Water vapor and oxygen permeability

165 The water vapor permeability (WVP) of the films was determined by using the ASTM

166 E96-95 (ASTM, 1995) gravimetric method, considering the modification proposed by

167 McHugh et al. (1993). Films were selected for WVP tests based on the lack of physical

168 defects such as cracks, bubbles, or pinholes. Distilled water was placed in Payne

169   permeability cups (3.5 cm diameter, Elcometer SPRL, Hermelle /s Argenteau, Belgium)

170   to expose the film to 100% RH on one side. Once the films were secured, each cup

171   was placed in a relative humidity equilibrated cabinet at 25 °C, with a fan placed on the

172   top of the cup to reduce resistance to water vapor transport. RH of the cabinets (53%)

173   was held constant using oversaturated solutions of magnesium nitrate-6-hydrate

174   (Panreac Química, SA, Castellar del Vallés, Barcelona). The cups were weighed every

175   1.5 h for 24 h by using an analytical scale (ME36S Sartorius, Germany, 0.0001 g). To

176   calculate the water vapor transmission rate, the slopes of the steady state period of the

177   curves of weight loss as a function of time were determined by linear regression. From

178   this data, water vapor permeability values were obtained, considering the average

179   value of film thickness in each case. The equation proposed by McHugh et al. (1993)

180   was used to correct the effect of concentration gradients established in the stagnant air

181   gap inside the cup.

182   The oxygen barrier capacity of the films was evaluated by measuring oxygen

183   permeability (OP) by means of an Ox-Tran 1/50 system (Mocon, Minneapolis, USA) at

184   25 °C (ASTM Standard Method D3985-95, 2002). Measurements were taken at 53%

185   RH in films previously equilibrated at the same RH. Films were exposed to pure

186   nitrogen flow on one side and pure oxygen flow on the other side. The OP was

187   calculated by dividing the oxygen transmission rate by the difference in the oxygen

188   partial pressure on the two sides of the film, and multiplying by the average film

189   thickness. At least three replicates per formulation were taken into account.

190

191   2.7. Optical properties

192   The transparency of the films was determined by applying the Kubelka–Munk theory

193   (Hutchings, 1999) for multiple scattering to the reflection spectra. When the light

194   passes through the film, it is partially absorbed and scattered, which is quantified by the

195   absorption (K) and the scattering (S) coefficients. Internal transmittance (T_i) of the films

196   was quantified using Equation (1). In this Equation R_0 is the reflectance of the film on

197   an ideal black background. Equation (2) and (3) are used to calculate a and b

198   parameters, respectively. R in equation 2 is the reflectance of the sample layer backed

199   by a known reflectance (R_g). The surface reflectance spectra of the films were

200   determined from 400 to 700 nm with a spectrocolorimeter CM-5 (Konica Minolta Co.,

201   Tokyo, Japan) on both a white and a black background. All measurements were

202   performed at least in triplicate for each sample on the free film surface during its drying.

203   In bilayer films, measurements were carried out on the CH layer.

204         $Ti = \sqrt{(a - R_0)^2 - b^2}$ (1)

205         $a = \frac{1}{2}\left(R + \frac{R_0 - R + R_g}{R_0 R_g}\right)$ (2)

206         $b = \sqrt{a^2 - 1}$ (3)

207

208   Color coordinates of the films, L^*, C^*_{ab} (Equation (4)) and h^*_{ab} (Equation (5)) from the

209   CIELAB color space were determined, using D65 illuminant and 10^0 observer, and

210   taking into account R_∞ (Equation 6), which is the reflectance of an infinitely thick layer of

211   the material.

212         $C^*_{ab} = \sqrt{a^{*2} + b^{*2}}$ (4)

213     $h^*_{ab} = arctg\left(\frac{b^*}{a^*}\right)$ (5)

214         $R_\infty = a - b$ (6)

215   Whiteness index (WI) was determined according to equation 7.

216

217         $WI = 100 - ((100 - L^*)^2 + a^{*2} + b^{*2})^{0.5}$ (7)

218

219   Gloss was measured using a flat surface gloss meter (MultiGloss 268, Minolta,

220   Langenhagen, Germany) at an angle of 60^0 with respect to the normal to the film

221   surface, according to the ASTM standard D523 (ASTM, 1999). Prior to gloss

222   measurements, films were conditioned at 25 ^{0}C and 53% RH for one week. Gloss

223   measurements were carried out over a black matte standard plate and were taken in

224   triplicate. Results were expressed as gloss units, relative to a highly polished surface of

225   standard black glass with a value close to 100. For bilayer films, gloss was measured

226   on the CH layer. For CH casted monolayer films, gloss measurements were performed

227   on the free film surface for water evaporation.

228

229   2.8. Antimicrobial properties

230   The antimicrobial capacity of the films (monolayers and bilayers) was tested in pork

231   meat, as described in previous studies (Bonilla et al., 2014). Films were put in contact

232   with the meat surface by the CH side. Sliced pork meat (about 10 g) was placed in petri

233   dishes (5 cm in diameter) to obtain the test samples. The surface of the meat slice was

234   coated with the films. Non-coated samples (control) and samples coated with the

235   different types of films were stored in duplicate at 10 ^{o}C for 7 days in a thermostat

236   cabinet (Aqualytic GmbH & Co, Dortmund, Germany).

237   To perform microbiological analyses, 10 g of each sample were aseptically obtained

238   and homogenized in a Stomacher (Bag Mixer 400, Interscience) with 90 mL of sterile

239   buffered peptone water for 2 min. Aliquots were serially diluted in buffered peptone

240   water and plated out following standard methodologies. Total aerobial and coliform

241   microorganism counts were determined at 0, 1, 4 and 7 days. Total aerobial counts

242   were determined in Plate Count agar incubated at 37 ^{0}C for 48 h. Coliform

243   microorganisms were determined in Violet Red Bile Agar incubated at 37 ^{0}C for 48 h.

244   All tests were performed in triplicate.

245

246   2.9. Statistical analysis

247   Statistical analyses were performed through analysis of variance (ANOVA) using

248   Statgraphics Centurion XVI- II. Fisher's least significant difference (LSD) procedure at

249   95 % was used.

250

251   **3. Results and discussion**

252   3.1 Microestructure

253   Figure 1 shows the FESEM micrographs of the cross-section bilayer films, where the

254   two polymer layers can be clearly distinguished. The estimated thickness of each

255   monolayer agreed with the initial values of the respective monolayers, thus maintaining

256   the 3:1 ratio for starch and chitosan layers. The micrographs showed very good

257   adhesion of both polymer layers and no detachment was observed, which confirmed

258   the good compatibility of polymers at the interface. CS:CH bilayers exhibited a

259   continuous homogeneous aspect at both phases, while starch layer showed some

260   micro-cracks, which are related with the more brittle nature of this film under the

261   observation conditions, (theoretical 0 water content), as reported by Jiménez, Fabra,

262   Talens, & Chiralt (2012) for starch films. Moreover, the absence of starch granules,

263   points to the effectiveness of shear and thermoprocessing at gelatinizing the starch

264   granules. In the CS:CH bilayers with oregano or clove essential oils, the oil droplets or

265   their voids created after cryofracture can be clearly distinguished in the CH layer.
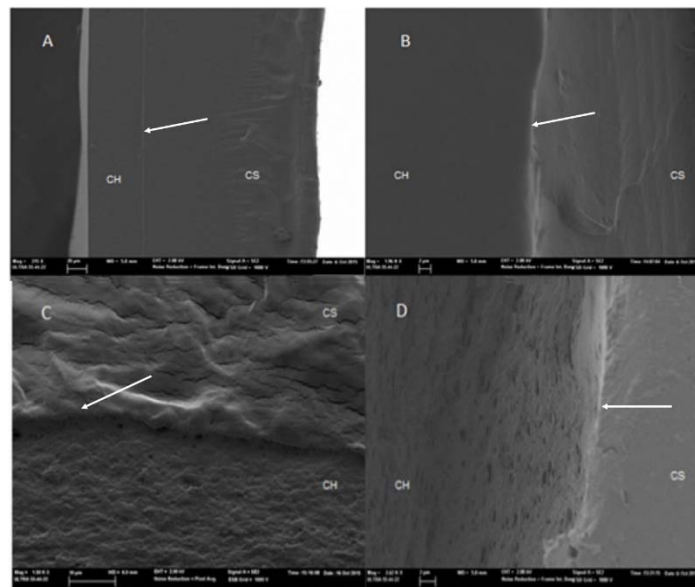

267   **Figure. 1.** FESEM micrographs of cross-sections of bilayer films A and B) CS-CH at

268   different magnifications C) CS-CH-OEO; D) CS-CH-CLEO. The arrow indicates the

269   layer interface.

270

271

272   3.2. Thermal characterization

273   The thermal degradation of the films was analyzed by TGA, which provides information

274   about the thermal stability of polymers and the potential effect of the essential oils

275   added, due to their potential diffusion into both layers and interactions with each

276   macromolecule (Ortega-Toro, Jiménez, Talens, & Chiralt, 2014). Figure 2 shows the

277   typical curves of the initial mass losses of the monolayers and bilayers, and the

278   derivative curves with the peaks associated with the different weight losses caused by

279   thermal degradation.
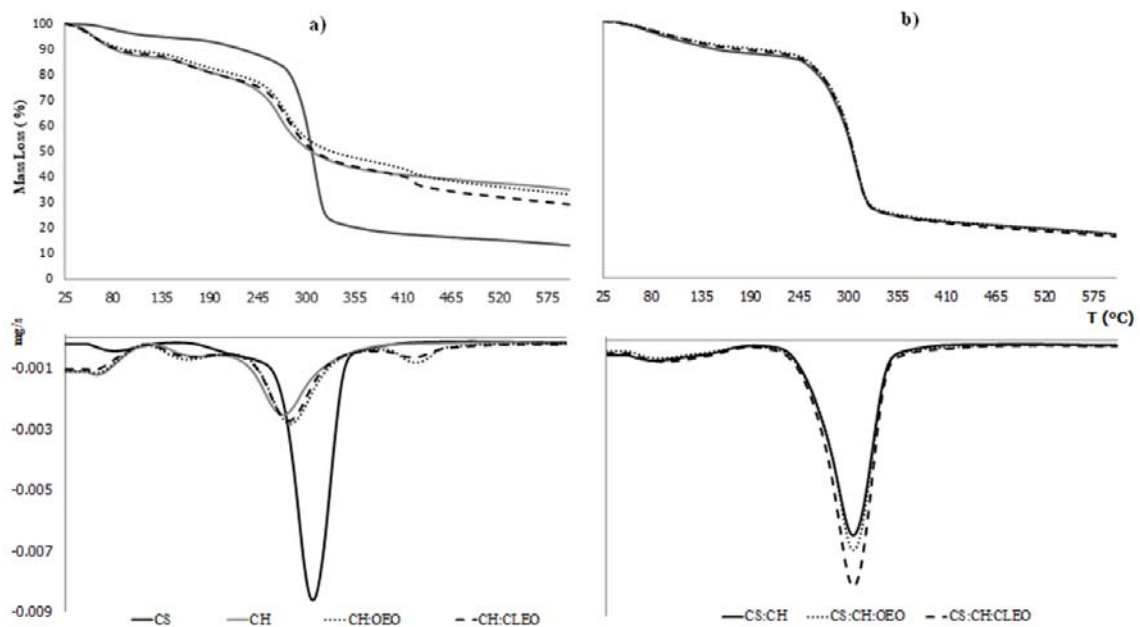
280

281   **Figure 2**. Typical thermogravimetric curves (weight loss vs. temperature) and first

282   derivative (mg/s vs temperature) for a) monolayer films and b) bilayer films.

283

284   All films exhibited weight loss below 130 ºC, which must be attributed to the loss of

285   adsorbed and bound water. By comparing monolayer samples, CH films exhibited

286   weight loss between 130-240 ºC (about 10%) regardless the presence of EO, which

287   could be due to the partial deamination of the chains at this temperature range (de

288   Brito & Campana-Filho, 2007). Afterwards, polymer chains degrade in a faster step

11

289   between 270ºC and 320 ºC showing a less sharp pattern than starch monolayers. T_{max}

290   of pure starch films was 308ºC, which is in accordance with previous studies (Dang &

291   Yoksan, 2015; Pelissari, Grossmann, Yamashita, & Pineda, 2009). In contrast, T_{max} of

292   CH monolayers was 269 ºC, near to that reported by other authors (Chen, Wang, Mao,

293   Liao, & Hsieh, 2008; Lewandowska, 2009; Tripathi, Mehrotra, & Dutta, 2009; Bonilla,

294   Talón, Atarés, Vargas, & Chiralt, 2013). As seen in Table 1, no great effect of the EO

295   was observed in the thermodegradation pattern of CH, except for the small loss (about

296   5%) that occurred at very high temperature (400-450ºC) and a slight increase in

297   temperature of the maximum degradation rate (T_{max}).

298

299   **Table 1**. Thermal properties of the films and the essential oils (T_0, T_{max}, Mass loss

300   during degradation). Mean values and standard deviation, in brackets.

Sample	T_0 (ºC)	T_{max} (ºC)	%Mass loss
CS	279.44 (0.18)[g]	308.40 (0.14)[h]	86.94 (0.01)[g]
CH	241.21 (0.05)[c]	269.13 (0.06)[c]	65.15 (0.01)[a]
CH:OEO	248.34 (0.42)[d]	276.49 (0.01)[e]	70.79 (0.02)[c]
CH:CLEO	247.4 (0.2)[d]	275.82 (0.01)[d]	67.07 (0.01)[b]
CS:CH	271.50 (0.17)[e]	308.05 (0.07)[g]	82.92 (0.06)[e]
CS: CH:OEO	274.4 (0.4)[f]	307.82 (0.02)[f]	82.81 (0.01)[d]
CS:CH:CLEO	274.6 (0.4)[f]	307.81 (0.03)[f]	83.84 (0.02)[f]
OEO	131.2 (0.9)[a]	151.09 (0.12)[a]	82.83 (0.01)[d]
CLEO	133.3 (0.6)[b]	171.75 (0.11)[b]	82.84 (0.01)[d]

301   Different superscripts letters (a-h) within the same column indicate significant differences among formulations ($p < 0.05$).

302

303   The small weight loss in films containing EO could be attributed to the losses of

304   strongly bonded molecules of the essential oils, which are delivered after the polymer

305   degradation. Phenolic compounds, such as the main of components of oregano and

306   clove essential oils, can crosslink with amino groups of the CH chains, becoming

307   bonded to the matrix (Pelissari et al., 2009; Reyes-Chaparro et al., 2015). This

308   behavior has been also observed by Ramos, Jiménez, Peltzer, & Garrigós (2012) and

309   Reyes-Chaparro et al. (2015) for essential oils included in CH matrix. No losses of free

310   essential oils compounds were observed at their volatilization temperature (150 ºC-170

311   ºC, Table 1), which could indicate that the main part of non-bonded compounds

312   evaporated during the film drying step by the steam distillation effect associated to the

313   water evaporation, as observed in previous studies for similar film composition

314   (Perdones, Chiralt, & Vargas, 2016). Table 1 shows the temperatures for initial and

315   maximum degradation rates of polymers, where the lower values of CH than those of

316   starch can be observed, as well as the small increase in T_{max} of CH films promoted by

317   essential oils. This effect could be due to the polymer bonding of the EO phenolic

318   compounds, which can slightly modify thermal resistance.

319   As concerns bilayer films, thermodegradation pattern was very similar and closer to

320   that of starch monolayer, in agreement with the greatest ratio of this polymer in the

321   films. The lack of appreciable differences due to the essential oils, as observed for CH

322   monolayers, can be related with the small weight fraction of the essential oil in the

323   double sheet. Nevertheless, an additional loss of essential oil compounds could occur

324   during the bilayer thermocompression, mainly due to the steam drag effect associated

325   to the residual water evaporation. Therefore, the processing parameters (temperature

326   and time) should be optimized to avoid excessive evaporation and loss of these

327   compounds incorporated (Dobkowski, 2006; Ramos et al., 2012).

328

329   **3.3   Mechanical properties**

330   As shown in Table 2, CS film exhibited the lowest elastic modulus and tensile strength

331   values and the highest elongation at break. In monolayer films, the addition of EOs to

332   CH films improved the stretchability and reduced the film stiffness. This effect can be

333   attributed to the developed interactions CH-phenolic compounds that weaken the CH

334   chain interaction forces, causing interruptions of the polymer chain aggregation in the

335   matrix, which favors the sliding of the chains during film stretching and reduce the

336   strength of the matrix (Bonilla, Atarés, Vargas, & Chiralt, 2012).

337

338   **Table 2.** Tensile properties (elastic modulus: EM, tensile strength: TS and elongation:

339   ε, at break) of the films. Mean values and standard deviation, in brackets.

Film	EM (MPa)	TS (MPa)	ε (%)
CS	565 (12)[a]	17.3 (0.4)[a]	7.5 (0.3)[f]
CH	1521 (52)[f]	51 (5)[f]	4.7 (0.3)[c]
CH:OEO	1078 (21)[d]	40 (3)[d]	6.2 (0.5)[e]
CH:CLEO	1417 (27)[e]	43 (3)[e]	5.9 (0.4)[d]
CS:CH	921 (80)[c]	20(2)[c]	2.28 (0.14)[b]
CS: CH:OEO	910 (38)[b]	17 (1)[a]	1.9 (0.2)[a]
CS:CH:CLEO	918 (4)[d]	18(2)[b]	2 (2)[b]

340 Different superscripts (a-f) within the same column indicate significant differences among formulations (*$p < 0.05$).

341

342 The obtained values for pure CH monolayers were similar to those previously reported

343 by Bonilla et al. (2012) and Vargas, Perdones, Chiralt, Cháfer, & González-Martínez

344 (2011), while the incorporation of OEO and CLEO provoked similar effects to that

345 previously observed by Bonilla et al. (2012) for CH films containing basil or thyme

346 essential oils. The discontinuities introduced in the chitosan matrix by oil droplets

347 (Figure 1C and 1D), will also contribute to the loss of the film cohesion and mechanical

348 resistance.

349 All bilayer films showed higher values of EM and TS than CS monolayers, but lower

350 than the CH monolayer. Likewise, they exhibited lower extensibility than pure CS films

351 and CH-based monolayers, especially when the CH layer contained essential oils. This

352 behavior demonstrated the reinforcement effect produced by CH monolayer in the

353 prevalently starch films, despite its lower ratio in the double sheet. However, bilayers

354 lost flexibility probably due to the controlling effect of the CS-CH interface at film

355 fracture. The strong CS-CH bonding at the interface could make the chain sliding at

356 this zone difficult, provoking film fracture instead of plastic deformation. In this sense,

357 the enhanced film extensibility by EO was not evidenced in thermo-compressed

358 bilayers since the interfacial adhesion of the monolayers controlled the film fracture.

359 Nevertheless, with the CH layer adhesion, starch films gained stiffness and resistance

360 to fracture.

361

362 3.4   Film thickness and barrier properties

Table 3 shows the thickness values of the monolayer and bilayer films. Film thickness of the CH monolayers slightly decreased when OEO or CLEO was incorporated into the film formulation (from 66 µm to 52 µm), which is in accordance with the volatile losses during film formation since a similar total solid amount per surface unit was casted in all cases.

Table 3. Thickness, water vapor permeability (WVP) and oxygen permeability (OP) of the films. Mean values and standard deviation, in brackets.

Films	Thickness (µm)	WVP (g mm kPa^{-1} h^{-1} m^{-2})	OP (cm^{3}m^{-1}s^{-1} Pa^{-1}) x 10^{-13}
CS	171 (5)[c]	9.38 (0.11)[f]	0.601(0.009)[b]
CH	66 (3)[b]	5.35 (0.14)[a]	0.781 (0.01)[c]
CH:OEO	54 (3)[a]	6.9 (0.2)[d]	-
CH:CLEO	55 2[a]	5.9 (0.3)[b]	-
CS:CH	221 (5)[e]	7.3 (0.6)[c]	0.097 (0.003)[a]
CS: CH:OEO	209 (10)[d]	8.03 (0.18)[e]	-
CS:CH:CLEO	207 (9)[d]	7.87 (0.14)[e]	-

Different superscripts (a-f) within the same column indicate significant differences among formulations (*$p<0.05$).

A reduction in film thickness due to essential oil addition was previously reported in similar studies, and it was explained by important losses of essential oils during the drying step of the films, mainly due to the steam distillation effect associated to water evaporation (Perdones et al., 2016). Because of this, the thickness of the bilayers that incorporated EO were also slightly lower than that of CS:CH bilayer. Nevertheless, no significant flow of the polymer layers occurred during the thermocompression step, as revealed by the final bilayer thickness, which was close to the sum of the respective monolayers. FESEM observations (Figure 1) corroborate that in bilayer films the thickness of each film layer practically maintained its initial value, being the CS:CH proportion about 3:1. In fact, the low temperature applied in thermocompression (100 ºC) would not justify the polymer flow. However, at this temperature the residual water content of the film layers could evaporate also leading to losses of the EOs by steam distillation effect.

386   Table 3 also shows the barrier properties of the films. CH-based monolayer films

387   showed the lowest WVP values, and the addition of essential oils (OEO or CLEO)

388   slightly increased the WVP of CH films. This effect was also observed by Bonilla et al.

389   (2012) and Vargas, Albors, Chiralt, & González-Martínez (2009), and was attributed to

390   the loss of CH matrix cohesion associated to the chain interactions with the essential

391   oil compounds. As expected, bilayer films exhibited values of WVP between those

392   found for CS and CH monolayers, and essential oils also slightly promoted an increase

393   in the WVP values of bilayer films. As previously reported by Bonilla et al. (2013), the

394   oxygen permeability of pure CS and CH films was very low, but the oxygen barrier

395   properties of CS:CH bilayers were ever more improved with respect to CS or CH

396   monolayers. This effect could be due to the polymer interactions at the interface, which

397   generate a perpendicular layer to mass transfer in the bilayer, with great resistance to

398   the gas transport.

399

400   3.5   Optical properties

401   Figure 3 shows the spectral distribution curves of the internal transmittance (T_i) of the

402   monolayer and bilayer films.

403
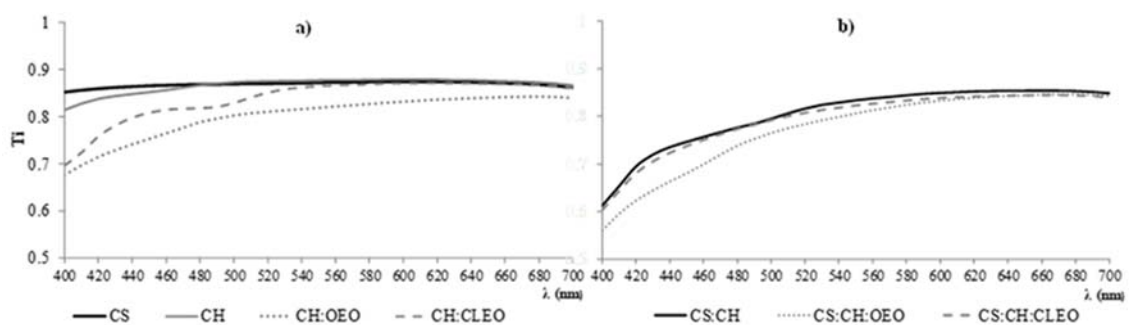
404

405   **Figure 3.** Spectral distribution curves of internal transmittance (T_i) of the (a) monolayer

406   and (b) bilayer films.

407

The results obtained revealed significant differences between films. CS monolayer was the most transparent, whereas CH monolayers showed a higher opacity, especially when they contained essential oils, whose dispersion in the matrix promotes light scattering, thus reducing film transparency to a different extent depending on the essential oil. Oregano EO led to greater reduction in transparency than cinnamon leaf EO, according to the different refractive index and coloration of their constituents, which provoke light selective absorption. As expected, bilayer films were less transparent, since an additional change in the film refractive index occurs at the polymer interface, enhancing light scattering.

From the reflectance spectra of an infinite film thickness, lightness (L^*), hue (h^*_{ab}), chroma (C^*_{ab}) and whiteness index (WI) of each film were calculated (Table 4). CS films showed higher lightness and WI than CH monolayers. The incorporation of essential oils led to a significant reduction in both WI and lightness values of CH films and yielded films with a yellower, more saturated color (lower hue values and higher chroma). This affected both mono and bilayer films. Therefore, bilayer films were darker than CS monolayers with a more saturated yellowish, especially when incorporated essential oils.

Table 4. Lightness (L^*), chroma (C^*_{ab}), hue (h^*_{ab}), whiteness index (WI) and gloss at 60º. Mean values and standard deviation, in brackets.

Films	L^*	C^*_{ab}	h^*_{ab}	WI	Gloss
CS	86.4 (0.7)[d]	5.4 (0.4)[a]	81 (2)[c]	84.9 (0.2)[e]	41 (2)[e]
CH	68 (1)[c]	10.2 (0.6)[b]	106.9 (0.6)[f]	66.4 (0.9)[d]	49 (2)[g]
CH:OEO	63.3 (0.4)[a]	17.64 (0.12)[c]	88.2 (0.2)[e]	59.1 (0.4)[b]	54 (1)[h]
CH:CLEO	63.5 (0.5)[a]	18.6 (0.3)[d]	88.7 (0.2)[e]	59.1 (0.3)[b]	47 (2)[f]
CS:CH	70.9 (0.5)[d]	25.4 (0.6)[f]	79.9 (0.4)[b]	61.4 (0.5)[c]	23 (0.)[a]
CS:CH:OEO	66.06 (0.8)[b]	26.83 (0.13)[g]	77.4 (0.5)[a]	57 (1)[a]	26 (1)[c]
CS:CH:CLEO	69 (2)[c]	22.7 (0.5)[e]	83.1 (0.7)[d]	62 (1)[c]	23 (2)[a]

Different superscripts (a-h) within the same column indicate significant differences among formulations (*$p < 0.05$).

The gloss of the films is linked to the morphology of their surface and generally, the smoother the surface, the glossier the film. Table 4 shows the gloss values at 60º of all

432 monolayer and bilayer films. Incorporation of essential oils did not notably affect the

433 gloss of the CH monolayers despite their potential effect on the film surface

434 morphology due to their dispersed nature in the films, which could increase the surface

435 roughness (Bonilla et al., 2012).

436 Thermo-compression in bilayers, greatly reduced the gloss of the CH face, which can

437 be attributed to the rearrangement of the chains near the surface, where temperature

438 reaches the highest value, provoking a less oriented and more disordered chain

439 arrangement and affecting the surface roughness.

440

441 **3.6   Antimicrobial properties**

442 Figure 4 shows the progress over storage time (up to 7 days) of coliform counts in non-

443 coated and coated pork meat.

444 CH monolayers were the most effective at reducing the growth of total aerobial and

445 coliform microorganisms during the whole storage period, and the growth inhibition

446 coincides with that previously reported by Bonilla et. al (2014).

447 The incorporation of essential oils into the CH monolayer films caused a slight increase

448 in the microbial counts. This indicates that CH was more effective than the essential

449 oils, at their final concentration in the films, in inhibiting the bacterial growth. The

450 reduction in the effective ratio of chitosan in the films that contain essential oils explains

451 the decrease in the antimicrobial effectiveness caused by a dilution effect (Sánchez-

452 González, Chiralt, González-Martínez, & Cháfer, 2011).

453 Bilayer films were slightly less effective than CH monolayers at controlling the bacterial

454 growth, especially at the end of incubation time, where more marked differences

455 between films were observed. The loss of antimicrobial capacity of CH in bilayers could

456 be due to the partial deamination of the CH chains during the thermocompression step,

457 as deduced from the thermal analysis. TGA of the bilayers do not exhibit the CH weight

458 loss occurred in CH monolayers between 130-200 ºC, which could indicate that this

459 event occurred during the film processing. Several authors indicated the role of amino

18

460   groups in the antimicrobial activity of CH (Kong, Chen, Xing, & Park, 2010; Verlee,

461   Mincke, & Stevens, 2017).
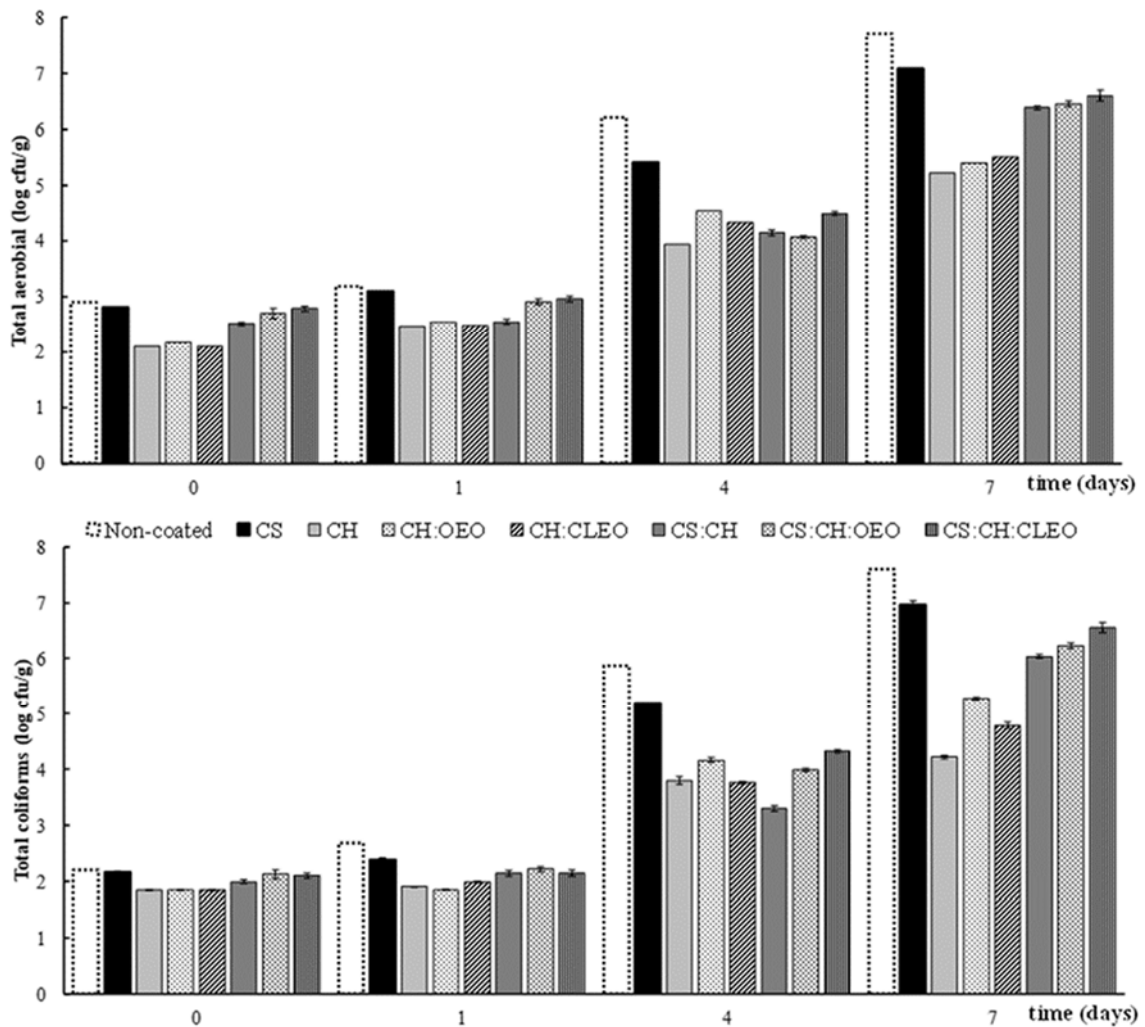
462

463

464   **Figure 4**. Total aerobial and coliform counts of non-coated minced pork samples and

465   samples coated with the films. Mean values and standard deviation.

466

467   At the end of storage, all films led to a reduction in microbial load as compared to non-

468   coated samples and samples coated with pure CS films, revealing the antimicrobial

469   action of CH, affected to a different extent by the dilution effect in the matrix and

470   thermal treatment.

471

4. Conclusion

It was possible to obtain starch-chitosan bilayer films, containing or not essential oils in the chitosan layer, by thermo-compression, exhibiting a good interfacial adhesion between the polymer layers. Starch-chitosan bilayer films showed better mechanical resistance than starch monolayers, although they were less stretchable due to the interfacial control of the film fracture. Bilayer films were slightly less transparent but showed acceptable optical properties. Chitosan was effective at controlling the bacterial growth in sliced pork meat. However, the thermal treatment used to obtain the bilayers reduced its effectiveness, revealing the loss of amino groups during treatment, as it was also confirmed by thermal analyses. Essential oils did not exhibit antimicrobial action in chitosan mono and bilayers when applied to pork meat. The final amount of essential oils in the films could be very limited by the potential losses occurred during the casting and thermoprocessing methods that were used for film production. Other strategies to incorporate the antimicrobial essential oils in the films should be used in order to improve the final retention of essential oils in polymer matrices and their effective release into the food media to exceed the minimally inhibitory concentration.

References

20

498   **1.** ASTM (1995). Standard test methods for water vapor transmission of materials. In

499   Standards designations: E96-95. Annual book of ASTM standards, (pp. 406 - 413).

500   Philadelphia, PA: American Society for Testing and Materials.

501   2. ASTM (1999). Standard test method for specular gloss. Standard Designations:

502   D523. In Annual book of ASTM standards. Philadelphia, PA: American Society for

503   Testing and Materials.

504   3. ASTM (2001). Standard test method for tensile properties of thin plastic sheeting. In

505   Standard D882 Annual book of American standard testing methods, (pp. 162 -

506   170). Philadelphia, PA: American Society for Testing and Materials.

507   4. ASTM (2002). Standard test method for oxygen gas transmission rate through

508   plastic film and sheeting using a coulometric sensor. Standard Designations: 3985-

509   95. In Annual book of ASTM standards. Philadelphia, PA: American Society for

510   Testing and Materials.

511   5. Atarés, L., Bonilla, J., & Chiralt, A., (2010). Characterization of sodium caseinate-

512   based edible films incorporated with cinnamon or ginger essential oils. *Journal of*

513   *Food Engineering*, 100, 678–687.

514   6. Avérous, L., Moro, L., Dole, P., & Fringan, C. (2000). Properties of thermoplastic

515   blends: starch–polycaprolactone. *Polymer*, 41, 4157 – 4167.

516   7. Avérous, L., Fringant, C., & Moro, L.(2001). Starch-Based Biodegradable Materials

517   Suitable for Thermoforming Packaging. *Starch/Stärke*, 53, 368 – 371.

518   8. Ayala-Zavala, J., Soto-Valdez, H., González-León, A., Álvarez-Parrilla, E.,

519   MartínBelloso, O., & González-Aguilar, G. (2008). Microencapsulation of cinnamon

520   leaf (*Cinnamomum zeylanicum*) and garlic (*Allium sativum*) oils in -cyclodextrin.

521   *Journal of Inclusion Phenomena and Macrocyclic Chemistry*, 60, 359 - 368.

522   9. Bakkali, F., Averbeck, S., Averbeck, D., & Idaomar, I. (2008). Biological effects of

523   essential oil sea review. *Food and Chemical Toxicology*, 46,446 - 475.

524   10. Bonilla, J., Talón, E., Atarés, L., Vargas, M., & Chiralt, A. (2013). Effect of the

525   incorporation of antioxidants on physicochemical of wheat starch–chitosan films.

526   *Journal of Food Engineering*, 118 (3), 271 - 278.

527   11. Bonilla, J., Atarés, L., Vargas, M., & Chiralt, A. (2014). Physical, structural and

528   antimicrobial properties of poly vinyl alcohol – chitosan biodegradable films. *Food*

529   *Hydrocolloids*, 35, 463 – 470.

530   12. Bonilla, J., Vargas, M., Atarés, A., & Chiralt, A. (2014). Effect of Chitosan Essential

531   Oil Films on the Storage-Keeping Quality of Pork Meat Products. *Food and*

532   *Bioprocess Technology*, 7, 2443 - 2450.

533   13. Burt, S. (2004). Essential oils: their antibacterial properties and potential

534   applications in foods—a review. *International Journal of Food Microbiology,* 94, 223

535   – 253.

536   14. Chang, S., Chen, P., & Chang, S. (2001). Antibacterial activity of leaf essential oils

537   and their constituents from *Cinnamomum osmophloeum. Journal of*

538   *Ethnopharmacology*, 77, 123 – 127.

539   15. Chen, C. H., Wang, F. Y., Mao, C. F., Liao, W. T., & Hsieh, C. D. (2008). Studies of

540   chitosan: II. Preparation and characterization of chitosan/poly (vinyl alcohol)/ gelatin

541   ternary blend films. *International Journal of Biological Macromolecules*, 43, 37 - 42.

542   16. De Sousa J. P., de Azerêdo G. A., de Araújo Torres R., da Silva Vasconcelos M.

543   A., da Conceição M. L., & de Souza E. L. (2012). Synergies of carvacrol and 1,8-

544   cineole to inhibit bacteria associated with minimally processed vegetables.

545   *International Journal of Food Microbiology* 154, 145 – 151.

546   17. De Brito, D., & Campana-Filho, S.P. (2007). Kinetics of the thermal degradation of

547   chitosan. *Thermochimica Acta*, 465, 73 - 82.

548   18. Doane, W., Swanson, C., & Fanta,G. (1992). Emerging polymeric materials based

549   on starch- *ACS Symposium Series*, 476, 197 – 230.

550   19. Dutta, P.K., Dutta, J., & Tripathi, V.S. (2004).Chitin and chitosan : Chemistry ,

551   properties and applications. *Journal of Scientific & Industrial Research*, 63, 20 - 31.

552 20. Flores, S., Costa, D., Yamashita, F., Gerschenson, L., & Grossmann Eiras, M.

553 (2010). Mixture design for evaluation of potassium sorbate and xanthan gum effect

554 on properties of tapioca starch films obtained by extrusion. *Materials Science &*

555 *Technology*, 30(1), 196 - 202.

556 21. Ghanbarzadeh, B., & Oromiehi, A. R. (2009). Thermal and mechanical behavior of

557 laminated protein films. *Journal of Food Engineering*, 90,517 – 524.

558 22. Hutchings, J. B. (1999). Food color and appearance (2nd Ed.). Gaithersburg,

559 Maryland, USA: Aspen Publishers, Inc.

560 23. Jiménez, A., Fabra, M. J., Talens, P., & Chiralt, A. (2012). Effect of re-crystallization

561 on tensile, optical and water vapour barrier properties of corn starch films

562 containing fatty acids. *Food Hydrocolloids*, 26, 302 – 310.

563 24. Khan, B., Bilal Khan Niazi, M., Samin, G., & Jahan, Z. (2017). Thermoplastic Starch:

564 A Possible Biodegradable Food Packaging Material—A Review. *Journal of Food*

565 *Process Engineering*, 40, e12447.

566 25. Kim, H., Park, S., & Park, H. (2004). Inactivation of *Escherichia coli* O157:H7 by

567 cinnamic aldehyde purified from *Cinnamomum cassias* hoot. *Food Microbiology*,

568 21, 105 – 110.

569 26. Kong, M., Chen, X.G., Xing, K., & Park, H.J. (2010). Antimicrobial properties of

570 chitosan and mode of action: A state of the art review. *International Journal of Food*

571 *Microbiology*, 144, 51 - 63.

572 27. Lertsutthiwong, P., Ng, C., Chandrkrachang, S., & Stevens,W. (2002). Effect of

573 chemical treatment on the characteristics of shrimp chitosan, *Journal of Metals*,

574 *Materials and Minerals*, 12, 11 – 18.

575 28. Lewandowska, K. (2009). Miscibility and thermal stability of poly(vinyl alcohol)/

576 chitosan

577 29. mixtures. *Thermochimica Acta*, 493, 42 - 48.

578 30. López, O., Garcia, A., Villar, M., Gentili, A., Rodriguez, M., Albertengo, L. (2014).

579 Thermo-compression of biodegradable thermoplastic corn starch films containing

580 chitin and chitosan. *Food Science and Technology*, 57, 106 106 - 1515.

581 31. Lv F., Liang H., Yuan Q., & Li C. (2011). *In vitro* antimicrobial effects and

582 mechanism of action of selected plant essential oil combinations against four food-

583 related microorganisms. *Food Research International*, 44, 3057 – 3064.

584 32. Mali, S., Grossmann, M. V., García, M., Martino, M., & Zaritzky, N. (2006). Effects

585 of controlled storage on thermal, mechanical and barrier properties of plasticized

586 films from different starch sources. *Journal of Food Engineering*, 75, 453 - 460.

587 33. Mc Hugh, T. H., Avena-Bustillos, R., & Krochta, J. M. (1993). Hydrophobic edible

588 films: modified procedure for water vapour permeability and explanation of

589 thickness effects. *Journal of Food Science*, 58, 899 - 903.

590 34. Naushad Emmambux, N., & Stading, M. (2007). *In situ* tensile deformation of zein

591 films with plasticizers and filler materials. *Food Hydrocolloids*, 21, 1245 – 1255.

592 35. Ortega-Toro, R., Jiménez, A., Talens, P & Chiralt, A. (2014). Properties of starch-

593 hydroxypropyl methylcellulose based films obtained by compression molding.

594 *Carbohydrate Polymers*, 109, 155 - 165.

595 36. Park, I., Lee, H., Lee, S., Park, J., & Ahn, Y. (2000). Insecticidal and fumigant

596 activities of Cinnamomum cassia bark-derived materials against *Mechoris ursulus*

597 (Coleoptera: Attelabidae). *Journal of Agriculture and Food Chemistry*, 48, 2528 –

598 2531.

599 37. Pelissari, F. M., Yamashita, F., García, M. A., Martino, M. N., Zaritzky, N. E., &

600 Grossmann, M. V. E. (2012). Constrained mixture design applied to the

601 development of cassava starch-chitosan blown films. *Journal of Food Engineering*,

602 108, 262 – 267.

603 38. Perdones, A., Vargas, M., Atarés, L. & Chiralt, A. (2014). Physical, antioxidant and

604 antimicrobial properties of chitosan - cinnamon leaf oil films as affected by oleic

605 acid. *Food Hydrocolloids*, 36, 256 – 264.

606   39. Ramos, M., Jiménez, A., Peltzer, M., & Garrigós, M. C. (2012). Characterization

607   and

608   40. antimicrobial activity studies of polypropylene films with carvacrol and thymol for

609   active packaging. *Journal of Food Engineering*, 109, 513 - 519.

610   41. Reyes-Chaparro, P., Gutierrez-Mendez,N., Salas-Muñoz,E., Ayala-Soto,J.G.,

611   Chavez-Flores, D., & Hernández-Ochoa, L. (2015). Effect of the Addition of

612   Essential Oils and Functional Extracts of Clove on Physicochemical Properties of

613   Chitosan-Based Films. *International Journal of Polymer Science*, 714, 254 - 260.

614   42. Sánchez-González, L., Chiralt, A., González-Martínez, C., & Cháfer, M. (2011).

615   Effect of essential oils on properties of film forming emulsion and films based on

616   hydroxypropylmethylcellulose and chitosan. *Journal of Food Engineering*, 105, 246

617   - 253.

618   43. Shogren, R. (1998). Starch: Properties and Materials Applications. In Biopolymers

619   from renewable resources (Ed. D. L.Kaplan), Springer-Verlag, Berlin, pp. 30–46.

620   44. Swanson, C. L., Shogren, R. L., Fanta, G. F., & Imam, S. H. J. (1993). Starch-

621   plastic materials-Preparation, physical properties, and biodegradability (a review of

622   recent USDA research). *Journal of Environmental Polymer Degradation*, 1,155 -

623   166.

624   45. Singh, G., Maurya, S., de Lampasona, M. P., & Catalan, C. A. N. (2007). A

625   comparison of chemical, antioxidant and antimicrobial studies of cinnamon leaf and

626   bark volatile oils, oleoresins and their constituents. *Food and Chemical Toxicology*,

627   45, 1650 – 1661.

628   46. Singh, H., Srivastava, M., Singh, A., & Srivastava, A. (1995). Cinnamon bark oil, a

629   potent fungitoxicant against fungi causing respiratory tract mycoses. *Allergy*, 50,

630   995 – 999.

631   47. Tomka, I. (1991). Thermoplastic starch. *Advances in Experimental Medicine and*

632   *Biology*, 302, 627 – 637.

633 48. Thunwall, M., Boldizar, A., & Rigdahl, M. (2006). Compression molding and tensile

634   properties of thermoplastic potato starch materials. *Biomacromolecules*, 7, 981 -

635   986.

636 49. Van Soest, J.J.G. (1996). Starch plastics structure-property relationships. P&L

637   Press, Wageningen, Germany/ Utrecht University (Netherland).

638 50. Vangalapati, M., Satya, S. N., Prakash, D. V. S., & Avanigadda, S. (2012). A review

639   on pharmacological activities and clinical effects of cinnamon species. *Research*

640   *Journal of Pharmaceutical, Biological and Chemical Sciences*, 3, 653 – 663.

641 51. Vargas, M., Albors, A., Chiralt, A., & González-Martínez, C. (2009).

642   Characterization of chitosan-oleic acid composite films. *Food Hydrocolloids*, 23,

643   536-547.

644 52. Vargas, M., Perdones, A., Chiralt, Cháfer, M., & González-Martínez, C. (2011).

645   Effect of homogenization conditions on physicochemical properties of chitosan-

646   based film-forming dispersions and films. *Food Hydrocolloids*, 25, 1158-1165.

647 53. Verlee, A., Mincke, S., & Stevens, C.V. (2017). Recent developments in

648   antibacterial and antifungal chitosan and its derivatives. *Carbohydrate Polymers*,

649   164,268-283.

650 54. Weska, R., Moura, J., Batista, L., Rizzi, J., & Pinto, L. (2007). Optimization of

651   deacetylation in the production of chitosan from shrimp wastes: use of response

652   surface methodology, *Journal of Food Engineering*, 80, 749 – 753.

653 55. Xu, Y. X., Kimb, K. M., Hanna, M. A., & Nag, D. (2005). Chitosan- starch composite

654   film: preparation and characterization. *Industrial Crops and Products*, 21,185 - 192.

655 56. Youn, D., No, H., & Prinyawiwatkul, W. (2007). Physical characteristics of

656   decolorized chitosan as affected by sun drying during chitosan preparation,

657   *Carbohydrate Polymers*, 69, 707 –712.

658 57. Zobel, H.F. (1988). Starch crystal transformations and their industrial importance.

659   Starch/Stärke, 40, 1-7.

660

661